Zeolites

DOI: 10.1002/ange.200501250

Water Condensation in Hydrophobic Nanopores**

Nicolas Desbiens, Isabelle Demachy, Alain H. Fuchs, Helène Kirsch-Rodeschini, Michel Soulard, and Joël Patarin*

There are many intriguing situations in everyday life where water is confined to spaces of nanoscopic dimensions by hydrophilic as well as hydrophobic substrates such as in colloidal particles,[1–4] protein cavities,[5] and inorganic solid walls.[6,7] Fundamental interest stems from the fact that the properties of confined water are believed to be very different from those of the corresponding bulk fluid at the same temperature and chemical potential.[8–11] Recently, it was shown that storage or dissipation of mechanical energy could be achieved by forced intrusion/extrusion of water into/from hydrophobic porous materials.[12–14] Intrusion of water into silicalite-1 zeolite at a hydraulic pressure of about 100 MPa at room temperature results in its condensation. A spontaneous capillary evaporation (drying) took place upon release of the pressure. Similar behavior was observed very recently in the case of hydrophobized MCM-41 mesoporous materials.[15] Interestingly, the intrusion/extrusion cycle was accompanied by a hysteresis effect in the latter case, but not in the former one. Situations were also encountered in which no extrusion of water took place upon release of the pressure (zeolite β and wide-pore MCM-41).[12–15] To shed light on these phenomena we have undertaken a molecular simulation study of the intrusion/extrusion of water into/from hydrophobic silicalite-1 zeolite. Some new experimental data are also reported. We have been able to reproduce, for the first time to our knowledge,the spontaneous condensation of water that is observed experimentally, and thus to investigate the properties of confined water in these hydrophobic nanopores at the molecular level.

The intrusion/extrusion process was investigated with silicalite-1 by using two different experimental devices. The same silicalite-1 sample, prepared according to a literature method,[12] was used in both cases. In the first device the water/silicalite-1 system was placed in a cell of variable volume (1.20 cm^3 under atmospheric pressure) which was immersed in an oil-containing vessel able to withstand very high hydrostatic pressure. The volume changes were determined at constant temperature by increasing the pressure progressively, as described in reference [16]. The compressibility curve obtained corresponds to that obtained by Eroshenko et al.[12,14] (Figure 1; dashed line). The method used in this first set of experiments is believed to be accurate for determining the water intrusion pressure, but the absolute

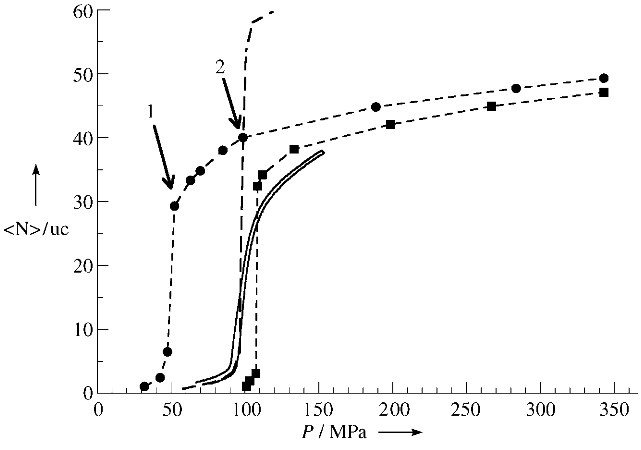

Figure 1. Condensation/drying isotherms of liquid water in silicalite-1 at 300 K. Solid line (displaying hysteresis): experimental data (this study); dashed line: experimental data;[12] circles: simulated isotherms with a silicon atomic charge of 1.4 a.u.; squares: simulated isotherm with a silicon atomic charge of 1.2 a.u. (see text). The dotted lines are a guide to the eye.

---

[*] N. Desbiens, Dr. I. Demachy, Prof. Dr. A. H. Fuchs
Laboratoire de Chimie Physique
CNRS and Université Paris-Sud
91405 Orsay (France)
Fax: (+33) 1-6915-6188
E-mail: fuchs@lcp.u-psud.fr
Ir. H. Kirsch-Rodeschini, Dr. M. Soulard, Dr. J. Patarin
Laboratoire de Matériaux à Porosité Contrôlée
CNRS, École Nationale Supérieure de Chimie de Mulhouse and
Université de Haute-Alsace
68093 Mulhouse (France)

[**] Prof. Randy Snurr and Dr. Anne Boutin are gratefully acknowledged for fruitful discussions and correspondence.

intruded volume seems to be overestimated. A second set of experiments was therefore performed which made use of a modified Carlo Erba mercury porosimeter, and a more realistic volume was obtained. In this case, the cell containing the water/zeolite system consisted of a 2-cm^3 polypropylene cylinder sealed by a mobile piston. This cell was introduced into the 15-cm^3 glass cell of the porosimeter which was filled with mercury. The variation in volume was determined from the conductivity measurement, which depends on the mercury height in the capillary tube of the glass cell. The maximum volume change was about 0.5 cm^3. We believe this methodology provides a more accurate measurement of the volume than the preceding case. The corresponding experimental intrusion/extrusion data are reported in Figure 1 (solid line). It is interesting to note that a porous volume of 0.18 cm^3 per gram of zeolite is obtained from the experimental intruded volume at 150 MPa and using the average computed water density of approximately 0.6 kg m^{-3} (see below). This result is in complete agreement with the pore volume determined from nitrogen adsorption data.[12,13] This observation seems to demonstrate that the current volumetric data are much more accurate than the previously published ones. A very narrow hysteresis effect is observed during the intrusion/extrusion cycle; this effect was not observed in the first set of experiments. It is interesting to note that in a recent model proposed by Lefevre et al.,[15] it was predicted that the width of the intrusion/extrusion hysteresis in porous materials should progressively vanish as the pores get smaller. This prediction is in keeping with the current results.

We carried out Grand Canonical Monte Carlo (GCMC) simulations of the adsorption of water in silicalite-1. We used a rigid zeolite framework and used the atomic coordinates of the orthorhombic structure determined by Olson and et al.[17] We simulated a box of eight unit cells with periodic boundary conditions. We used the semiempirical TIP4P potential for water,[18] which was recently shown to provide a fairly good description of the adsorption of water in faujasite zeolites.[7,19] The host/guest potential is of the "Kiselev type":[20,21] It contains a single effective Lennard–Jones term that acts between the oxygen atoms of the framework and the oxygen atoms of the guest water molecules, together with a coulombic term that acts between the partial charges of the silicon and oxygen atoms and those of the guest molecules. We used the Lennard–Jones parameters for the zeolite oxygen atoms obtained from our previous work on the adsorption of hydrocarbons in silicalite-1[22] together with the Lorentz–Berthelot combining rules. The partial charge on the silicon atom was fixed at $+1.4$ a.u. (the zeolite oxygen atom bears a charge of -0.7 a.u. since the purely SiO_2 framework is neutral overall). There is an ongoing debate in the literature about the partial charge that a silicon atom should bear in silica-based materials; atomic charges have been reported in the range of 1.2 to 2.0 a.u., depending on the computational method used.[23–26] We found with the force-field model used here that the partial charge on the silicon atoms should be kept below approximately 1.7 a.u. for the silicalite-1 solid to exhibit hydrophobic character (namely, to prevent a capillary condensation phenomenon at a gas pressure below the saturation pressure of the bulk water). Details on this force-field adjustment will be reported elsewhere. We have chosen here the somewhat arbitrary value of 1.4 a.u. which corresponds to the Hartree–Fock calculation by Dovesi et al.[23] We have undertaken GCMC simulations of the adsorption of liquid water in silicalite-1. Thus, we have separately computed the relationship between the external pressure and the TIP4P chemical potential of liquid water at room temperature. GCMC simulations were then performed, at each pressure, by exchanging molecules between the zeolite sample and a fictitious external gas reservoir at the same chemical potential as the liquid water and at the pressure of interest. This method is similar to the one previously proposed by Snurr and coworkers for the adsorption of liquid alkanes.[27] Details of the GCMC algorithm and the statistical bias used can be found elsewhere.[22]

The adsorption data for the simulated liquid state at 300 K are reported in Figure 1. A stepwise condensation is observed at a pressure of about 50 MPa. The agreement with the experimental intrusion pressure is quite good, given that there is only a 3% difference in the chemical potential of liquid water between 50 and 100 MPa. An even better agreement with experimental data can be obtained by fixing an atomic charge of 1.2 a.u. on the silicon atom and -0.6 a.u. on each oxygen atom of the framework (Figure 1). The shape and the water loading of the computed intrusion isotherms are in good agreement with the currently reported experimental data. This observation is remarkable given the crudeness of the model used in the simulations. Simulations were also carried out using the MSPC/E semiempirical water potential model,[28] which is also known to reproduce quite well the saturation vapor pressure at room temperature. The computed adsorption curve (not shown here) was very similar to the TIP4P curve and also exhibited a stepwise, first-order-like condensation. This result is reminiscent of the two-state description of the water behavior in model carbon nanotubes[29] and nanoporous cylindrical channels[30] observed recently in molecular dynamics studies.

The computed isotherm shown in Figure 1 is reversible, within statistical uncertainties. This is generally what we expect for a Monte Carlo simulation, although it is known that GCMC adsorption isotherms may, in some special cases, exhibit hysteresis.[31] The computed isotherm displayed in Figure 1 can thus be considered as the equilibrium intrusion/extrusion curve of the model water/silicalite-1 system. It is the first time, to our knowledge, that this condensation/drying phenomenon has been reproduced theoretically.

We have examined in some detail the condensation mechanism in the molecular simulation model. The silicalite-1 framework (Figure 2) contains interconnected channels of pores of two types: straight channels which run in the direction of the *y*-axis and zigzag channels parallel to the *xz* plane. The Atlas of Zeolite structure types[32] denotes the silicalite-1 structure (MFI structure type) as being made of straight channels (SC) with a diameter of 5.4 Å, zigzag channels (ZC) with a diameter of 5.0 Å, and intersections (I). There are four SC, ZC, and I per unit cell, and they correspond to volume fractions of about 29, 33, and 38%, respectively. We have separately computed the local density of condensed water in these three subvolumes. This calcu-

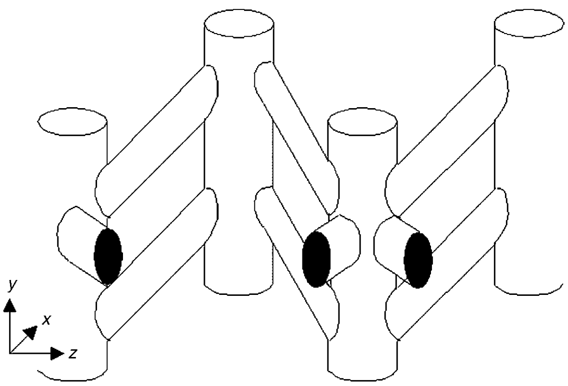

Figure 2. View of the interconnected pore channels in silicalite-1 (MFI-type structure).

lation is based on the determination of the void spaces in the zeolite model, which relies on a somewhat arbitrary definition of the "size" of the framework oxygen atoms. We have taken here a value of 1.5 Å for the van der Waals radius of the framework oxygen atoms. Consequently, the local density values shown in Figure 3, together with the average density and the bulk water density, depend on the criterion used for computing the void spaces, which leads to an uncertainty of about 10% in the estimates of these local density values. The trends however (for example, the ratio of the intersection/straight channels densities and the way it changes with pressure) depend only weakly on this criterion.

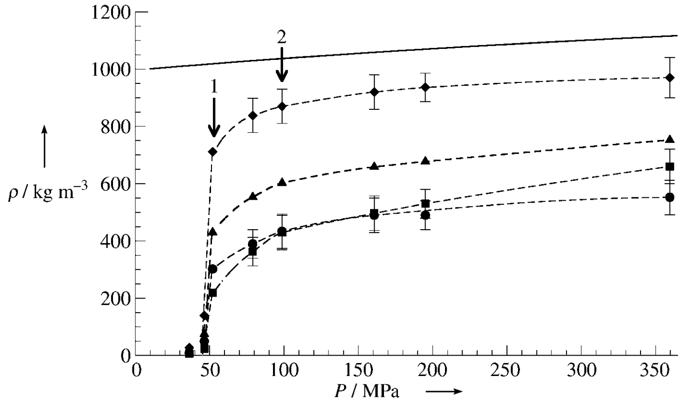

Figure 3. Density of condensed water in silicalite-1 as a function of pressure from GCMC simulations. Squares: local density in the zig-zag channels (ZC). Circles: local density in the straight channels (SC). Diamonds: local density in the intersections (I). Triangles: average water density in silicalite-1. Solid line: bulk water density. The dotted lines are a guide to the eye. No error bars are displayed for the average densities, for reasons of clarity.

The stepwise condensation phenomenon is observed in all three regions of the zeolite at a pressure of approximately 50 MPa. At this pressure (marked "1" in Figures 1 and 3) the average density of the condensed water is less than half that of the bulk water density under the same thermodynamic conditions. The condensed fluid is extremely inhomogeneous. The density in the intersections is three times as large as that of the fluid in the straight or zigzag channels. The average occupancy is 5 water molecules at an intersection, while there are only 1.5 molecules on average in the SC or ZC. At this stage, the filling of the channels (SC or ZC) is also highly inhomogeneous. Some of the sections of the channels are empty, while others contain 2–3 molecules. There is clearly a clustering effect in this first condensation step. The formation of water clusters in silicalite-1 was already suggested in some previous molecular dynamics studies.[33–35] The same behavior seems to hold true in the case of carbon nanopores.[36,37] The current results are in keeping with the observation of Vaitheeswaran et al.[37] that linear chains of water molecules inside a narrow cylindrical pore are less stable than the water clusters in a spherical nonpolar cavity of comparable volume.

A second condensation regime takes place as the pressure is increased from 50 to about 100 MPa. At the point marked "2" in Figures 1 and 3, each intersection is now occupied by six molecules and the SC and ZC by two water molecules. The channel filling now becomes homogeneous, with each channel section containing approximately the same number of molecules. At this stage, the water density in the intersection has reached 85% of the bulk fluid value, while the density in the channels is lower by a factor of two.

A progressive filling of the silicalite-1 nanopores is observed upon pressure increases above 100 MPa. Given the uncertainties in the density calculations, it is hard to tell whether or not the density at the intersections reaches the bulk value at a sufficiently high pressure. However, it seems clear that the water density in the channels is always lower by a factor close to two. This fact can be interpreted by considering that the 3D-like geometry of the pore intersections enables water molecules to pile up in more or less the same way as in the bulk liquid. On the other hand, the pseudo-1D channel geometry prevents such a bulklike state from being reached. It is worth mentioning that the strong depletion of fluid observed in these simulations cannot simply be accounted for by a failure of the water force-field. The TIP4P intermolecular potential was checked to provide very accurate values for the density of bulk water at high pressure.

The observed water depletion is attributed to the hydrophobic (nonwetting) character of the purely siliceous nanopores studied here. Silicalite-1 zeolite consists of a three-dimensional network of SiO_4 tetrahedra connected to each other through shared oxygen atoms. This arrangement enables the build up of a purely siliceous open framework material without surface defects (bond breaking, presence of silanol groups).[12] Conversely, amorphous silica surfaces are highly defective, and thus display hydrophilic character. This is the case, for example, for the mesoporous MCM-41 materials. Hydrophobicity is generated in MCM-41 by covalent grafting of nonpolar siloxane chains.[15] In a recent study Engemann et al.[38] reported experimental evidence of interfacial melting of ice in contact with amorphous silica. The authors observed a quasiliquid layer with an enhanced density ($\rho \approx 1.2$) relative to bulk water. This fact can be tentatively attributed to the hydrophilic character of the amorphous silica surface.

One lesson that can be learned from this study is that simple models and simulation methods found useful for studying gas adsorption in nanoporous materials can be extended to describe the intrusion/extrusion cycle of a nonwetting fluid in a hydrophobic solid. We have reproduced for the first time the condensation transition of water in silicalite-1 zeolite at room temperature. The condensation process disclosed by computer simulations is much more complex than initially expected from the intrusion/extrusion experiments. The picture of water confined to hydrophobic spaces of nanoscopic dimensions that emerges from this study is one of a strongly depleted and highly inhomogeneous fluid.

Received: April 9, 2005

Keywords: adsorption · molecular modeling · phase transitions · water · zeolites

---

[1] P. Ball, *Nature* **2003**, *423*, 25–26.
[2] J. W. G. Tyrell, P. Attard, *Phys. Rev. Lett.* **2001**, *87*, 176104-1–176104-4.
[3] R. Steitz, T. Gutberlet, T. Hauss, B. Klösgen, R. Krastev, S. Schemmel, A. C. Simonsen, G. H. Findenegg, *Langmuir* **2003**, *19*, 2409–2418.
[4] D. Chandler, *Nature* **2002**, *417*, 491–491.
[5] B. Yu, M. Blaber, A. M. Gronenborn, G. M. Clore, D. L. D. Caspar, *Proc. Natl. Acad. Sci. USA* **1999**, *96*, 103–108.
[6] J. H. Walther, R. L. Jaffe, E. M. Kotsalis, T. Werder, T. Halicioglu, P. Koumoutsakos, *Carbon* **2004**, *42*, 1185–1194.
[7] C. Beauvais, A. Boutin, A. H. Fuchs, *ChemPhysChem* **2004**, *5*, 1791–1793.
[8] T. M. Truskett, P. G. Debenedetti, S. Torquato, *J. Chem. Phys.* **2001**, *114*, 2401–2418.
[9] P. Gallo, M. A. Ricci, M. Rovere, *J. Chem. Phys.* **2002**, *116*, 342–346.
[10] A. Giaya, R. W. Thompson, *J. Chem. Phys.* **2002**, *117*, 3464–3475.
[11] I. Brovchenko, A. Geiger, A. Oleinikova, *J. Chem. Phys.* **2004**, *120*, 1958–1972.
[12] V. Eroshenko, R.-C. Regis, M. Soulard, J. Patarin, *J. Am. Chem. Soc.* **2001**, *123*, 8129–8130.
[13] V. Eroshenko, R.-C. Regis, M. Soulard, J. Patarin, *C. R. Phys.* **2002**, *3*, 111–119.
[14] M. Soulard, J. Patarin, V. Eroshenko, R.-C. Regis, Proceedings of the 14th International Zeolite Conference, Cape Town (Eds.: E. Van Steen et al.), **2004**, pp. 1830–1837.
[15] B. Lefevre, A. Saugey, J. L. Barrat, L. Bocquet, E. Charlaix, P. F. Gobin, G. Vigier, *J. Chem. Phys.* **2004**, *120*, 4927–4938.
[16] V. Eroshenko, A. Fadeev, *Colloid J.* **1995**, *57*, 446–449.
[17] D. H. Olson, G. T. Kokotailo, S. L. Lawton, W. M. Meier, *J. Phys. Chem.* **1981**, *85*, 2238–2243.
[18] W. L. Jorgensen, J. Chandrasekhar, J. D. Madura, R. W. Impey, M. L. Klein, *J. Chem. Phys.* **1983**, *79*, 926–935.
[19] C. Beauvais, A. Boutin, A. H. Fuchs, *Adsorption* **2005**, in press.
[20] A. Bezus, A. V. Kiselev, A. A. Lopatkin, P. Q. Du, *J. Chem. Soc. Faraday Trans. 2* **1978**, *74*, 367–379.
[21] A. H. Fuchs, A. K. Cheetham, *J. Phys. Chem. B* **2001**, *105*, 7375–7383.
[22] P. Pascual, P. Ungerer, B. Tavitian, P. Pernot, A. Boutin, *Phys. Chem. Chem. Phys.* **2003**, *5*, 3684–3693.
[23] R. Dovesi, C. Pisani, C. Roetti, B. Silvi, *J. Chem. Phys.* **1987**, *86*, 6967–6971.
[24] L. Uytterhoeven, W. J. Mortier, P. Geerlings, *J. Phys. Chem. Solids* **1989**, *50*, 479–486.
[25] H. Heinz, U. W. Suter, *J. Phys. Chem. B* **2004**, *108*, 18341–18352.
[26] a) A. V. Larin, D. P. Vercauteren, *Int. J. Inorg. Mater.* **1999**, *1*, 201–207; b) A. V. Larin, L. Leherte, D. P. Vercauteren, *Chem. Phys. Lett.* **1998**, *287*, 169–177.
[27] S. Chempath, J. F. M. Denayer, K. M. A. De Meyer, G. V. Baron, R. Snurr, *Langmuir* **2004** *20*, 150–156.
[28] G. C. Boulougouris, I. G. Economou, D. N. Theodorou, *J. Phys. Chem. B* **1998**, *102*, 1029–1035.
[29] a) G. Hummer, J. C. Rasaiah, J. P. Noworyta, *Nature* **2001**, *414*, 188; S. Vaitheeswaran, J. C. Rasaiah, G. Hummer, *J. Chem. Phys.* **2004**, *121*, 7955–7965.
[30] R. Allen, J.-P. Hansen, S. Melchionna, *J. Chem. Phys.* **2003**, *119*, 3905–3919.
[31] F. Porcheron, P. Monson, *Langmuir* **2004**, *20*, 6482–6489.
[32] Atlas of zeolite Framework types http://www.iza-structure.org. Ch. Baerlocher, W. M. Meier, D. H. Olson, *Atlas of Zeolite Framework Types*, 5th rev. ed., Elsevier, Amsterdam, **2001**.
[33] P. Demontis, G. Stara, G. B. Suffritti, *J. Phys. Chem. B* **2003**, *107*, 4426–4436.
[34] C. Bussai, S. Fritzsche, R. Haberlandt, S. Hannonghua, *J. Phys. Chem. B* **2003**, *107*, 12444–12450.
[35] K. S. Smirnov, D. Bougeard, *Chem. Phys.* **2003**, *292*, 53–70.
[36] T. Ohba, H. Kanoh, K. Kaneko, *J. Phys. Chem. B* **2004**, *108*, 14964–14969; T. Ohba, H. Kanoh, K. Kaneko, *Nano Lett.* **2005**, *5*, 227–230.
[37] S. Vaitheeswaran, H. Yin, J. C. Rasaiah, G. Hummer, *Proc. Natl. Acad. Sci. USA* **2004**, *101*, 17002–17005.
[38] S. Engemann, H. Reichert, H. Dosch, J. Bilgram, V. Honkimäti, A. Snigirev, *Phys. Rev. Lett.* **2004**, *92*, 205701.